

**Avalanches in the draining of nanoporous Nuclepore mediated by the superfluid helium film**

M. P. Lilly,\* A. H. Wootters, and R. B. Hallock

*Laboratory for Low Temperature Physics, Department of Physics, University of Massachusetts, Amherst, Massachusetts 01003*

(Received 12 July 2001; published 11 February 2002)

When capillary-condensed superfluid  $^4\text{He}$  drains from pore spaces in the nanoporous material Nuclepore, the fluid drains in a series of large-scale avalanches in which substantial numbers of pores (up to  $\sim 2.5\%$  of the sample) drain as a single cooperative event. In this work we document the behavior of such avalanches in a number of different multiple-detector configurations in an effort to investigate the origin of the interactions among the pores that lead to the avalanche behavior. We conclude that the presence of a superfluid  $^4\text{He}$  film on the surface of the Nuclepore plays a significant role in causing the avalanche behavior. We also investigate aspects of the spatial distribution of pores that are involved in an avalanche event, and conclude that avalanche events involve pores that are distributed over the entire sample; avalanches do not typically involve a high-density cluster of pores in a local region of the substrate.

DOI: 10.1103/PhysRevB.65.104503

PACS number(s): 67.70.+n, 47.55.Mh, 67.40.Hf, 68.43.Mn

**I. INTRODUCTION**

If one studies the cyclic adsorption and desorption of helium from the porous material Nuclepore, one observes a hysteretic behavior.<sup>1,2</sup> Film thickness growth is followed by capillary condensation; then, upon reduction of the chemical potential, one observes a rather steep draining curve as the capillary condensed fluid in the pores drains. Nuclepore is a rather interesting material for such studies of nanocapillarity, in that it is populated by a relatively high density ( $\sim 3.5 \times 10^8$  pores/cm<sup>2</sup>) of rather well-defined nearly cylindrical pores. The use of superfluid helium for such studies provides a unique opportunity to explore the draining behavior that is unencumbered by viscosity effects.

In an earlier papers<sup>1,3</sup> we showed that the hysteretic behavior of superfluid helium in Nuclepore is such that the draining part of the hysteresis curve is populated by avalanches. The avalanches observed correspond to  $\sim 2 \times 10^4$  to  $\sim 3 \times 10^7$  pores draining at one time (out of a sample consisting of  $\sim 1 \times 10^9$  pores). Our technique to make these measurements was described in substantial detail in earlier work,<sup>2,3</sup> and we will only briefly repeat the essence of it here. To make the relevant measurements we place an appropriate sample of Nuclepore in a sample cell, and control the chemical potential by controlling the sample temperature and/or the local  $^4\text{He}$  vapor pressure. The chemical potential is measured *in situ* by measurements of the time of flight of third sound. Third sound is a tidal-like wave that propagates on a thin film of superfluid helium.<sup>4</sup> The speed of a third sound wave is a sensitive measure of the local chemical potential. The extent to which the pores in the Nuclepore sample are filled with superfluid  $^4\text{He}$  is monitored by means of a capacitance technique.<sup>2,5</sup> Capacitor plates are evaporated on the two opposing sides of a  $10 \mu\text{m}$  thick 200-nm pore-diameter Nuclepore polycarbonate membrane, and measurements of the capacitance provide an appropriate measure of the filling fraction of the pores between the capacitor plates. The avalanche experiments that yielded the number of draining pores cited above only measured the number of pores draining between the capacitor plates used for the measurements, and do not directly probe the spatial extent over which an avalanche

occurs on the Nuclepore. For example, if an avalanche event involves  $N=10^6$  pores, and the event is local in the sense that all pores that drain are adjacent to one another, then this avalanche will occupy an area  $A=N/\rho=0.28 \text{ mm}^2$ , where  $\rho=3.5 \times 10^8$  pores/cm<sup>2</sup> is the number of pores per unit area for 200-nm pore-diameter Nuclepore. If the group of pores formed a less dense cluster, the spatial scale of the avalanche would be larger. In this paper we will report on experiments that are designed to provide information about the spatial scale of the avalanches on the Nuclepore substrate, and to provide insight into the mechanism by which pore-pore interactions take place. Such interactions must be present for pores to show avalanche behavior.

**II. DOUBLE CAPACITOR TECHNIQUE AND SPATIALLY EXTENDED AVALANCHES**

In an effort to gain insight into the spatial extent of the avalanches, we used a multiple-capacitor measurement technique. In this technique two or more capacitors are simultaneously monitored while the Nuclepore draining takes place. We begin with a description of the first such measurement, a measurement that utilized two capacitors on the same piece of Nuclepore.

The substrate used for the double capacitor measurements is shown schematically in Fig. 1. We evaporated 50 nm of Ag over two regions on each side of a piece of 200-nm pore-diameter Nuclepore to create two capacitors, denoted C1 and C2. These two capacitors each had plates of area  $4.8 \times 20.2 \text{ mm}^2$ , and were separated by 3.2 mm. Using a fast

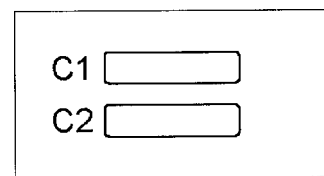


FIG. 1. Schematic view of a Nuclepore sample with two 50-nm-thick Ag capacitors located side by side. The two capacitors each had plates of area ( $4.8 \times 20.2 \text{ mm}^2$ ) and were separated by 3.2 mm.

switch controlled by a computer, a single Andeen Hagerling 2500A capacitance bridge was used to monitor both  $C1$  and  $C2$  sequentially. The system was typically prepared by completely filling the pores with liquid, and then reducing the chemical potential to the point where the pore draining was about to commence. To measure the avalanches,  $^4\text{He}$  was removed continuously from the sample chamber at a slow rate while a computer measured  $C1$ , toggled the switch (to  $C2$ ), measured the time, measured  $C2$ , and finally toggled the switch again (back to  $C1$ ). The complete measurement of the variables  $C1$  and  $C2$  and the time took a time interval of  $\sim 3$  sec, with four-sample (0.1-sec duration each) averaging on the capacitance bridge and  $\sim 7.5$  sec with eight-sample averaging. With this sequential measurement technique we were able to compare (within our measurement time) the time of occurrence of avalanches on capacitor  $C1$  to those on capacitor  $C2$ .

The main features to compare in the measurements of  $C1$  vs  $t$  and  $C2$  vs  $t$  are the times of occurrence of the avalanches and their sizes. If an avalanche occurs simultaneously on both capacitors, it must involve pores distributed over an area large enough to encompass at least part of each capacitor. If the event reaches beyond a capacitor plate, we do not observe the entire size of the event, but only the contribution of those pores located between the plates being monitored. If, on the other hand, an avalanche occurs on only one of the capacitors, we will conclude that it does not involve pores with a large enough spatial extent to extend to the second capacitor, i.e., in this case we would conclude that avalanche events are relatively local. In such a case, we might or might not be seeing the entire size of the event. As noted, the minimum possible spatial size of an avalanche that involves  $10^6$  pores occupies  $0.28 \text{ mm}^2$ . If this region (i.e., a high-density cluster of pores) were disk shaped ( $R = 0.30 \text{ mm}$ ), and it were to occur entirely on an area covered by capacitor  $C1$ , we would observe a substantial capacitance change on  $C1$  and observe nothing on  $C2$ . If it occurred on the edge of  $C1$ , a smaller step would be seen on  $C1$  and still nothing on  $C2$ , since the gap between the plates,  $3.2 \text{ mm}$ , is much larger than the presumed cluster dimension. The opposite extreme would be a spatially extended, low-density avalanche event, i.e., an avalanche caused by pores in dilute distribution located over a large portion of (or over all) of the Nuclepore substrate. If such an event were homogeneous, we would see simultaneous avalanches of equal size on both  $C1$  and  $C2$ . The double-capacitor results we shall describe provide us with the most basic test for learning about the distribution of pores involved in an avalanche. The first experiment to be described in this paper was designed to answer the question of whether avalanches are localized or are spatially extended.

The results for the draining of a 200-nm Nuclepore sample at  $T=1.451 \text{ K}$ , with two capacitors  $C1$  and  $C2$  present, are shown in Fig. 2. In Fig. 2(a), the complete draining for both capacitors is shown. The left data set represents data from capacitor  $C1$ , and the right data set represents data from capacitor  $C2$ . Note that although the two capacitors were essentially the same size, the capacitance values were a bit different. We attribute this to modest extra parallel capaci-

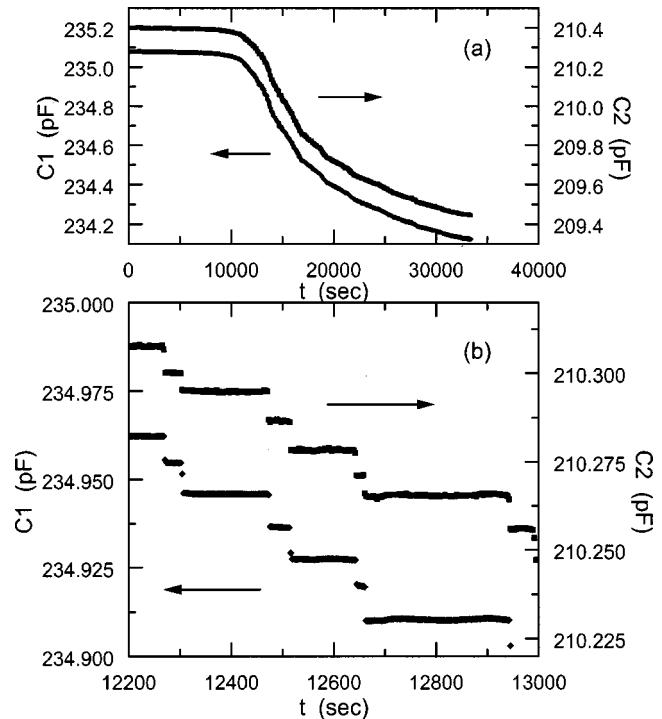


FIG. 2. Spatially extended avalanches at  $T=1.451 \text{ K}$  for 200-nm Nuclepore with double capacitors. The complete drainings  $C1$  (left, diamonds) and  $C2$  (right, squares) are shown in (a), and a close look at the avalanches (b) shows that these avalanche events are well correlated in size and time, and therefore must be spatially extended. The horizontal arrows in this and subsequent figures indicate which axis is appropriate to the relevant data set.

tance in one case relative to the other. As  $^4\text{He}$  was removed, and the chemical potential decreased, both  $C1$  and  $C2$  decreased together within our ability to time resolve the avalanches on the two capacitors. A magnification of several avalanches seen in the data of Fig. 2(a) is shown in Fig. 2(b). We see that within our time resolution the avalanches occurred at the same time, and involved steps of very similar sizes. This indicates that the avalanches were correlated, and therefore spatially extended. Thus the avalanche behavior seen in the draining of 200-nm pore-diameter Nuclepore does not arise from small local clusters of pores that drain together. Rather, it must consist of a distribution of pores spread in a relatively dilute fashion over the entire Nuclepore substrate; within our ability to time resolve the measurements (here  $\Delta t \sim 3$  sec), the avalanches are simultaneous. Such pores must interact in some manner if they are to drain in a single coordinated event.

Information about the pore distribution provides information concerning the potential interaction mechanisms that may be present. Suppose an avalanche consists of the draining of  $N$  pores contained within an area  $A$ . In this case, if we assume that the pores in an avalanche are distributed uniformly, then the distance between pores along the Nuclepore surface is  $l \sim (A/N)^{1/2}$ . In the case of a typical avalanche, e.g., one of the avalanches shown in Fig. 2(b), we find that  $l \sim 10 \mu\text{m}$ . This means that for avalanches of this size and smaller, the pores that drain will almost certainly not inter-

sect each other — they are too far apart for that to happen, given that the Nuclepore is  $10\ \mu\text{m}$  thick and the pores are tilted no more than  $34^\circ$  from the normal to the plane of the Nuclepore. Thus, for many of the observed correlated avalanches, many of which are smaller and represent pores that must be further apart, some mechanism of interaction must exist that does not require direct pore-pore contact. Large avalanches will involve pores closer together than this and may include pores that intersect, but small ones will predominantly involve pores that do not intersect.

We now compare, with more detail, the avalanche sizes observed on capacitor  $C1$  to those observed on capacitor  $C2$ . In order to measure the avalanche sizes for  $C1$  and  $C2$ , similar criteria for capacitance steps were used as in previous single capacitor experiments<sup>1,3</sup>: the size of the capacitance jump had to be larger than the noise on each measurement ( $0.0004\ \text{pF}$  on  $C1$  and  $0.0009\ \text{pF}$  on  $C2$  for the data of Fig. 2). The capacitance before and after a jump had to remain stable; we do not want to count any region where draining might be continuous. The duration of the jump had to be  $\leq 6\ \text{sec}$ . Finally, the size of the jump had to be larger than the measurement noise,  $\delta C$ . This resulted in a total of 96 avalanches on  $C1$ , and 79 on  $C2$ . Before any quantitative discussion of sizes, ratios, and correlation, we must caution that the capacitance switch used to enable the single capacitance bridge to measure both capacitors increased the noise in the capacitance measurement. This increase in noise was not associated with the switch until well after the data for this  $C1, C2$  measurement was taken. The switch introduced noise into both channels of measurement causing drifts in the capacitance with long periods ( $\geq 100\ \text{sec}$ ) and amplitudes of  $\sim 0.002\ \text{pF}$ . But, as we show in detail in Appendix A, this switch noise did not induce avalanches or contribute to the measured correlation between avalanche events on the two different capacitors.

The avalanche sizes for avalanche events observed on both capacitors  $C1$  and  $C2$  are shown in Fig. 3. The squares (solid and hollow) represent avalanches observed on capacitor  $C1$ , and the circles (solid and hollow) represent avalanches seen on  $C2$ . In order to test for correlation, we looked for avalanches on  $C1$  and  $C2$  that occurred at the same time. As noted earlier, the actual measurement is first to measure  $C1$ , then to measure the time, and finally to measure  $C2$ . Because of the time difference between measuring  $C1$  and  $C2$ , these simultaneous avalanches could occur either at the same time, or an avalanche could be seen first on  $C2$  and then in the next time step on  $C1$ . Close examination of the data in Fig. 2 indicates that both occurred. The correlated avalanches, 76 in all, are plotted with solid symbols, and the correlated pairs are connected by lines. The remaining uncorrelated avalanches are plotted with open symbols. This avalanche size plot is similar to those reported earlier<sup>1,3</sup> for 200-nm Nuclepore, in the sense that over the course of the draining the avalanches began small, increased in size, and then diminished. Because of the added noise due to the switch, we were not able to resolve the very small avalanches in these  $C1$  and  $C2$  experiments.

Note that the lines connecting the correlated avalanches in Fig. 3 are not vertical. Vertical lines would indicate that

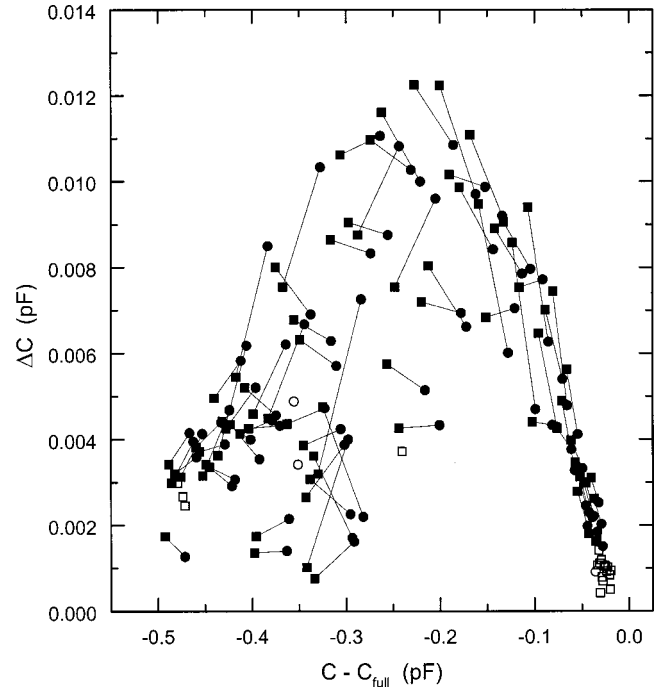


FIG. 3. Avalanches sizes for the data plotted in Fig. 2. Shown as a function of the deviation from “full” for each capacitor. The largest avalanches when the capacitors drained by  $\sim 0.25\ \text{pF}$  or  $\sim 20\%$ . The solid symbols represent avalanches that occurred at the same time on both  $C1$  (squares) and  $C2$  (circles). Lines connect the correlated pairs. The open symbols represent uncorrelated avalanches on  $C1$  (squares) and  $C2$  (circles).

when a correlated avalanche occurred, the same amount of  $^4\text{He}$  was previously drained from each capacitor. The slanted lines in Fig. 3 indicate that the draining on the two separate capacitors was not quite uniform. To show this better, we plot the difference in the capacitance values,  $C1 - C2$ , as a function of time as the draining progressed, in Fig. 4. The decrease in the difference between  $C1$  and  $C2$  shows that more fluid was draining from  $C1$  as the avalanches began ( $t \sim 10000\ \text{sec}$ ). After  $t \sim 14000\ \text{sec}$ , the difference began to increase, showing that the fluid draining rate in  $C2$  was higher. The reason for the asymmetry in the draining is not known. If the Nuclepore had an extended spatial inhomogeneity, a difference in the pore connectivity or size between the capacitors might cause different draining characteristics.

If the spatial extent of the avalanches were on the order of the size of the capacitor plates or smaller, then the actual size of the steps,  $\Delta C1$  and  $\Delta C2$ , might be quite different. If the avalanches were spatially distributed over a region much larger than the size of the capacitors, then  $\Delta C1 \sim \Delta C2$ . In Fig. 5, we plot the ratio of avalanche sizes for all avalanche pairs as a function of both the amount of  $^4\text{He}$  in the pores [ $\propto C1$ ; Fig 5(a)] and the size of one of the avalanches of each pair [ $\Delta C1$ ; Fig. 5(b)]. For either plot, most of the points are near  $\Delta C1/\Delta C2 \sim 1$ , with possibly a weak dependence<sup>7</sup> on  $C1$ , and no apparent dependence on  $\Delta C1$ . The mean and standard deviation of the ratios of the 76 correlated avalanches is  $\Delta C1/\Delta C2 = 1.08 \pm 0.33$ . Since most of the ratios are near 1 for simultaneous avalanche pairs, we

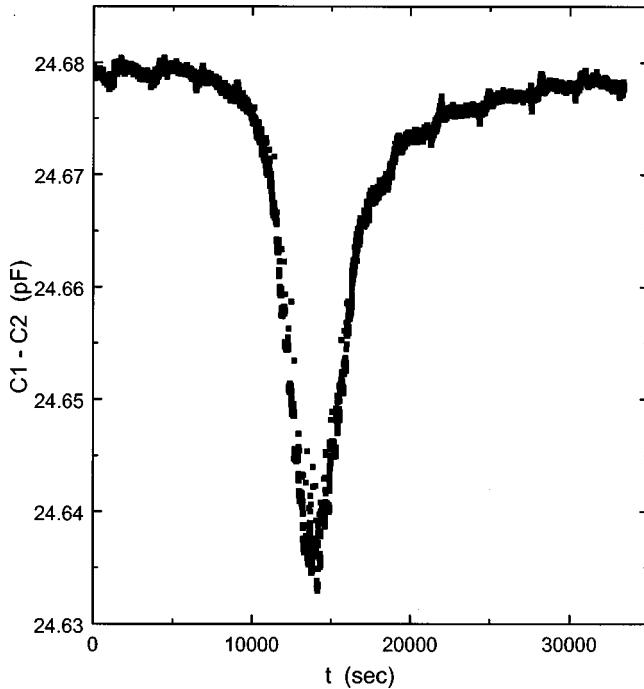


FIG. 4. Difference in capacitance values as draining occurred for  $C1$  and  $C2$  at  $T=1.451$  K. The individual measurements are shown separately in Fig. 2(a). If the capacitors drained uniformly,  $C1-C2$  would be constant. The decrease in the difference for  $10000 \text{ sec} \leq t \leq 14000 \text{ sec}$  shows that more  $^4\text{He}$  drained initially from  $C1$ . The draining from  $C1$  is slightly greater than that from  $C2$ .

conclude that the spatial size of the events is much larger than the size of the individual capacitor plates, i.e., an avalanche event spans both capacitor plates and most probably spans the entire Nuclepore sample. We will return to a discussion of correlated observations in a more quantitative manner shortly.

The observation of well-correlated avalanches allows us to conclude that the draining of  $^4\text{He}$  from Nuclepore is a spatially extended event. What mechanism causes these broadly distributed events? One possibility is that the percolated network of pores in Nuclepore is instrumental to the existence and propagation of avalanches. Computer simulation results<sup>1,2</sup> showed that the pores intersect in the material with a skewed distribution of intersections per pore averaging about five intersections per pore, resulting in the conclusion that the pore space is percolated. But, as we have seen earlier, for some avalanches the small size of the avalanche coupled with the observation of a correlation in time suggests that the draining pores are typically too far apart to intersect. A possible mechanism that does not require direct pore-to-pore contact is that a wave supported by the superfluid such as third or fourth sound couples pores over a long range. The physical picture is that the distortion of the meniscus of a filled pore caused by such a disturbance will stimulate that pore to drain. In order to learn more about the possibility of such an interaction, we constructed a sample with multiple capacitors on separate 200-nm Nuclepore substrates, and then joined them by use of a nonporous polycar-

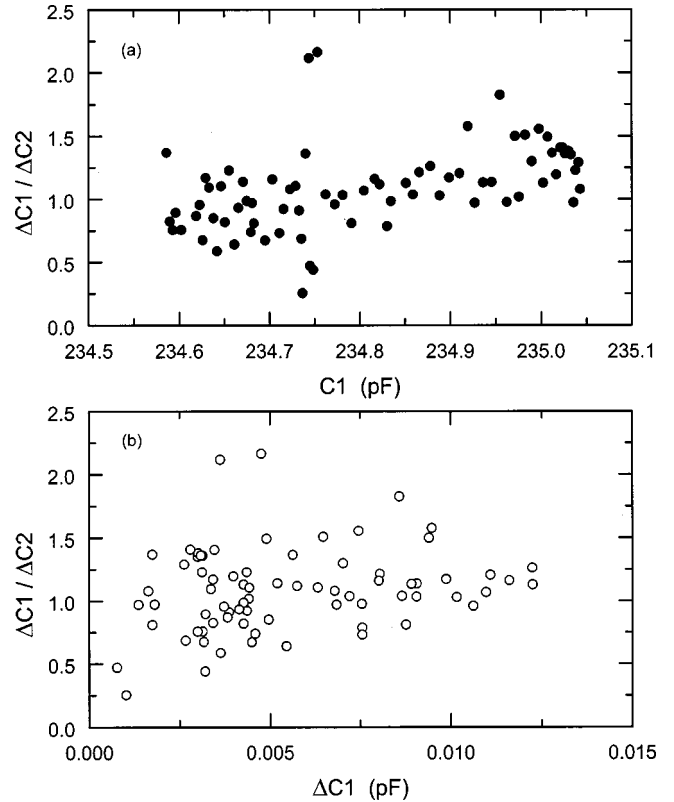


FIG. 5. The ratio of the correlated avalanche sizes as a function of the amount of  $^4\text{He}$  in the pores [ $C1$  (a)] and the avalanche size [ $\Delta C1$  (b)].

bonate patch<sup>8</sup>. The porous connection between capacitors was thus broken, but the  $^4\text{He}$  film connection still existed. We describe this experiment next.

### III. AVALANCHES WITHOUT A POROUS CONNECTION

A schematic diagram of the sample with this nonporous connection is shown in Fig. 6. The sample was created from two separate sheets ( $2.1 \times 2.5 \text{ cm}^2$ ) of 200-nm pore-diameter Nuclepore, 10  $\mu\text{m}$  thick, between which was placed a 0.25-cm-wide strip of nonporous Nuclepore, 6  $\mu\text{m}$  thick. The nonporous “Nuclepore” was acquired from the manufacturer of Nuclepore. The bottom of a second strip, 0.8 cm wide, of nonporous Nuclepore was covered with a thin film of Apizeon  $N$  grease, and pressed on top of the narrow strip. This is shown in the side view of Fig. 6. The wider strip overlapped both of the 200-nm Nuclepore sheets, and the grease joined all four pieces together. Before the grease could migrate, the sample was cooled to 77 K, freezing the grease into a glass-like state.<sup>8</sup>

Prior to the assembly of this multicomponent sample, several capacitors, third sound drivers, and transition-edge superconducting third sound detectors (thermometers) were evaporated on the two porous Nuclepore sheets. Each of the capacitors was  $0.76 \times 0.76 \text{ cm}^2 = 0.58 \text{ cm}^2$ . Of the four capacitors, leads were only connected to three capacitors  $C3$ ,  $C4$ , and  $C6$ , due to constraints imposed by the construction of the cryostat. By monitoring  $C4$  and  $C6$  (0.3-cm sepa-

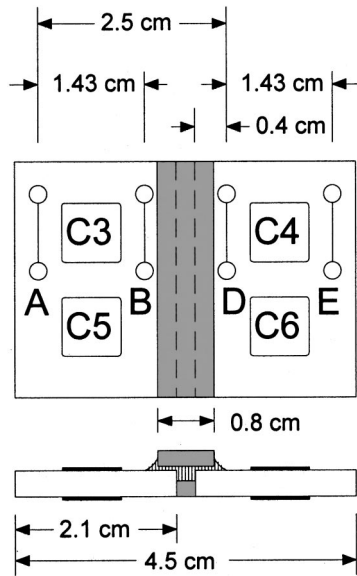


FIG. 6. Schematic diagram of the 200-nm Nuclepore sample connected with a nonporous strip. C3, C4, C5 and C6 are 50-nm-thick Ag capacitor plates. Strips A and E are 30-nm-thick Ag third sound drivers. Strips B and D are 30-nm-thick Al transition edge superconducting thermometers to detect third sound.

ration) simultaneously, we expected to reproduce the double capacitor results (i.e., from C1 and C2) described previously. By monitoring C3 and C4 (1.5-cm separation), we expected to be able to look for the presence of simultaneous avalanches across the nonporous strip. In addition to the capacitor for measuring the  $^4\text{He}$  in the pores, we also had the capability to drive (with electrodes A and E) and detect (with electrodes B and D) third sound pulses. The drivers were located (see Fig. 6)  $0.3 \pm 0.05$  cm from the outer edge,  $0.4 \pm 0.05$  cm from the small blank strip, 1.43 cm from the nearest detector (A-B, D-E), and  $2.5 \pm 0.05$  cm from the further detector (A-D, E-B). The third sound pulses had two primary purposes. First, driving a pulse at A and detecting across the strip at D (or driving E and detecting with B) would verify that the Apiezon N grease had properly created a bridge between the two Nuclepore porous sheets with a continuous  $^4\text{He}$  superfluid film connection. Second, with the ability to drive third sound, we would be able to tickle the system to perhaps modify the avalanche behavior; a fluctuation in the meniscus of a pore at its stability limit could be expected to cause that pore to drain.

In order to verify that the sample was intact at low temperatures and bridged by a superfluid film connection, we sent a third sound wave across the nonporous strip. The most sensitive thermometer, D, had a rather small but usable sensitivity of  $dR/dT = 120 \pm 10 \Omega/\text{K}$ . In Fig. 7, we show two data sets from this thermometer at  $T = 1.295$  K and helium film thickness  $d = 9.2$  layers (on glass). In Fig. 7(a), the pulse was generated at A, crossed the nonporous strip, and arrived at detector D (a total path length of 2.5 cm with 0.7 cm of this on the nonporous material and 1.8 cm on the porous Nuclepore). Since we could see the pulse, the film connection across the nonporous connection was intact. The total time of flight (A-D) of this pulse across the nonporous strip

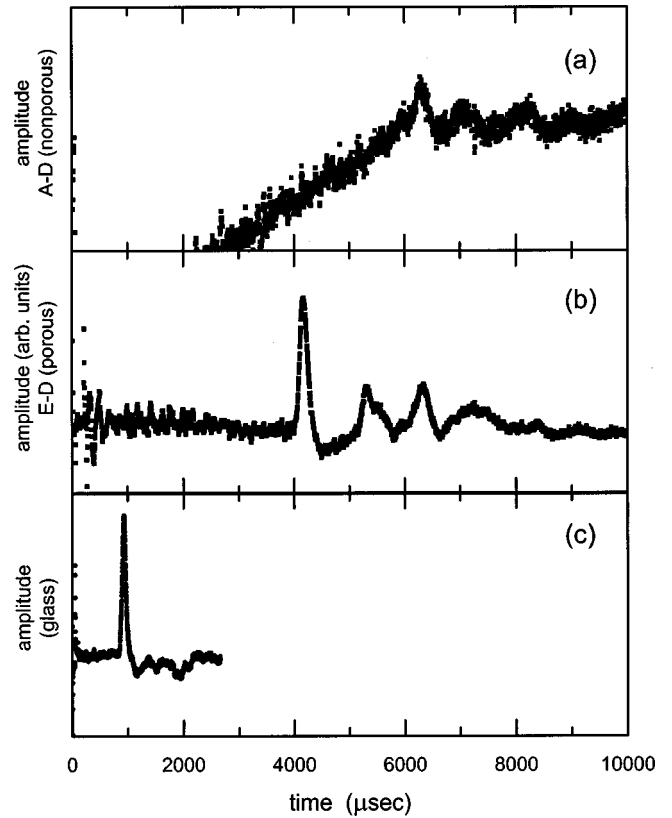


FIG. 7. Third sound time of flight measurements on Nuclepore and glass at  $T = 1.295$  K. In (a), the third sound generated at driver A crosses the nonporous strip and is detected by D. In (b), a direct pulse from driver E is detected at D. A number of reflections from the edges of the single Nuclepore sheet are also observed (see the text). In (c), we show a third sound pulse on a glass slide also located in the sample cell. The enhanced times of flight between (a), (b), and (c) are discussed in the text.

was  $\tau_{A-D} = 6100 \mu\text{sec}$ . In Fig. 7(b), the pulse was generated at driver E and arrived at D after a direct path (1.43 cm) across a single sheet of porous Nuclepore. The direct pulse arrived at  $\tau_{E-D} = 4160 \mu\text{sec}$ . The other pulses at longer times (5300, 6300, and 7250  $\mu\text{sec}$ ) were reflections from the edge near E and the edge at the nonporous strip. In Fig. 7(c), a third sound pulse on a separate substrate crossed 1.02 cm of glass in  $\tau_{\text{glass}} = 850 \mu\text{sec}$ . From the third sound velocity on glass of 1200 cm/sec we determined the film thickness on glass was approximately 9.2 layers.<sup>9</sup> The substantial difference in the velocity of third sound illustrated by the data in Fig. 7(a)–Fig. 7(c) has two origins. First, the propagation path difference for the third sound propagating from E to D is about 40% larger than the propagation path on the (smooth) glass substrate. The larger effect is the index of refraction for the propagation of third sound on the Nuclepore vs glass.<sup>10</sup> Together the  $^4\text{He}$  film thickness-dependent index of refraction and the differences in the propagation distance properly account for the differences in the third sound velocity. In Appendix B we discuss the presence and identification of the multiple peaks seen in the third sound data.

After verifying that the film connection was established,

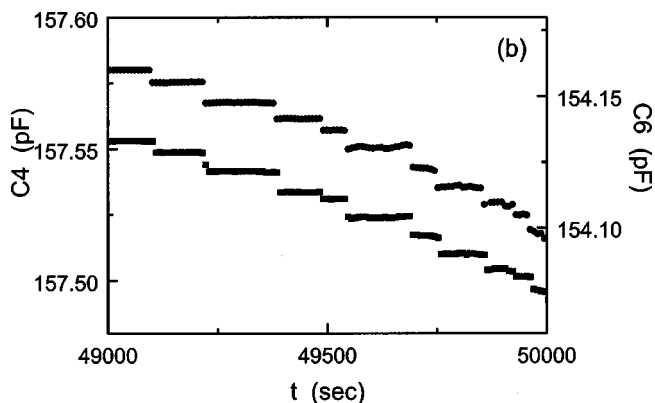


FIG. 8. Simultaneous avalanches on capacitors  $C4$  and  $C6$  at  $T=1.4246$  K. The data to the left (squares) is  $C4$  and the data to the right (circles) is  $C6$ . These results show the same sort of simultaneous avalanche events seen for  $C1$  and  $C2$  in Fig 2.

we conducted a sequence of several measurements at  $T=1.425$  K, near the temperature used for the double-capacitor ( $C1, C2$ ) experiment, and monitored  $C3$  and  $C4$  with the capacitance switch. Similar experiments were carried out by monitoring capacitors  $C4$  and  $C6$ , also with the switch in place. The results from the  $C4-C6$  experiment, shown in Fig. 8, indicate that, as expected, many of the avalanches were correlated, just as they were for the double-capacitor experiment ( $C1, C2$ ). The results from a separate experiment with measurements on  $C3$  and  $C4$  (Fig. 9) indicated that in spite of the absence of a porous pathway between the two capacitive detectors, there was still present a substantial number of correlated avalanche events seen on capacitors  $C3$  and  $C4$ . The presence of these correlated avalanches indicates that the *superfluid film*, which bridges the nonporous strip, was likely responsible for coupling the pores on either side; in the case of  $C3$  and  $C4$  avalanches direct pore-pore interconnections were not present.

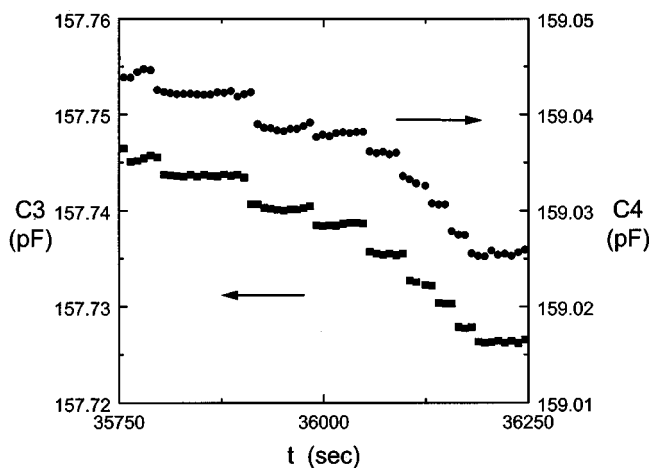


FIG. 9.  $C3$  and  $C4$  show correlated avalanches when the two separate sheets of Nuclepore were joined with a nonporous strip. The right axis ( $C3$ ) corresponds to the squares, and the left axis ( $C4$ ) corresponds to the circles. Note, due to the switching, that some of the simultaneous avalanches were measured on  $C2$  first, and in the next time step on  $C1$ .

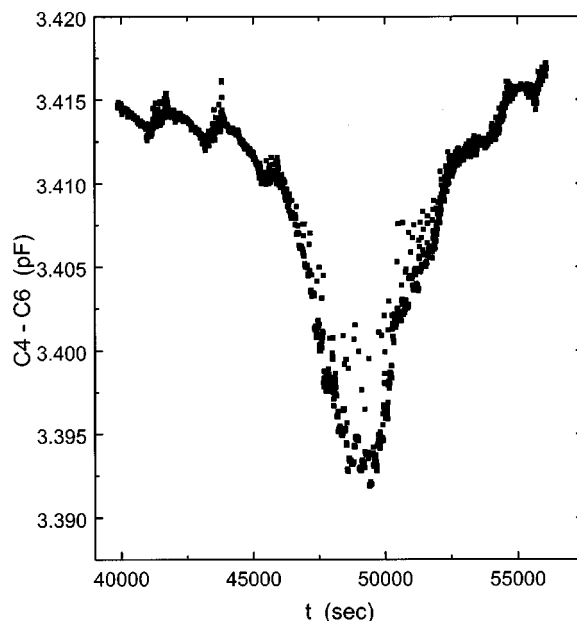


FIG. 10. Difference between the capacitors  $C4$  and  $C6$  at  $T=1.425$  K.

Recall that, previously, we observed a dip in the difference signal between the capacitance of  $C1$  and  $C2$  as draining occurred (Fig. 4). If we examine the difference between  $C4$  and  $C6$ , the two capacitors on the same sheet of Nuclepore, we again see a dip. This is shown in Fig. 10. In this case,  $C4$  initially drains faster than  $C6$ . This sample was from the same batch of Nuclepore (lot No. 0246), and mounted on the same frame. Either inhomogeneous pore structure<sup>11</sup> in the Nuclepore or perhaps the sample positioning on the Cu frame could be possible explanations for the asymmetric draining. Note, however, that just as in the previous case, the differences (0.025 pF, maximum) are very small compared to the total change in capacitance (0.65 pF).

In order to verify whether these simultaneous avalanches between  $C3$  and  $C4$  were really due to the film, rather than to an external trigger (i.e., were an artifact due to some sort of experimental perturbation), we modified the sample at the end of the experiment and conducted a final experiment with the modified sample to test for this possibility. After warming up the composite sample (with the nonporous bridge intact), we removed the nonporous Nuclepore bridge, resulting in the complete separation of the two pieces of Nuclepore. The two capacitors  $C3$  and  $C4$  were now on two disconnected pieces of Nuclepore,<sup>12</sup> and the separate samples were immediately cooled in proximity in the same sample cell. The disconnected substrates were tested for avalanches at  $T=1.4027$  K. In Fig. 11, we show a portion of the region where most of the draining occurs. Here avalanches on  $C3$  and  $C4$  were still present but no longer correlated. At the initial and final stages of draining, several small jumps in the capacitance did occur at the same time, indicating some sensitivity to disturbances. This is not surprising, since very long term fluctuations in the draining certainly depend on the external environment. However, where we observed the largest

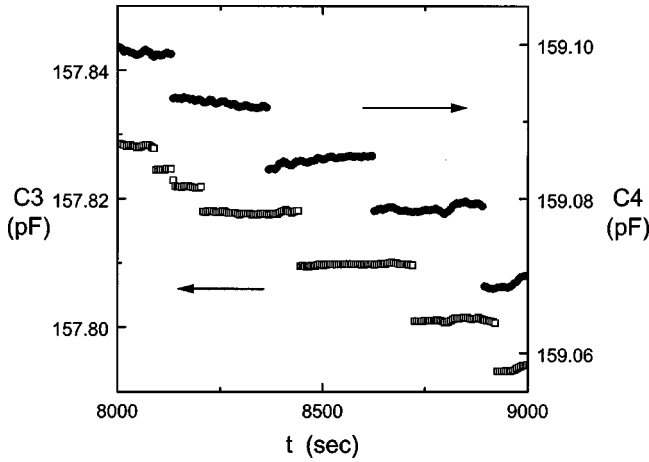


FIG. 11. The avalanches observed on  $C3$  and  $C4$  were completely uncorrelated when the two sheets of Nuclepore were separated by removing the nonporous strip. The right axis ( $C3$ ) corresponds to the squares, and the left axis ( $C4$ ) corresponds to the circles.

avalanches, no correlation was present; this is precisely the region where the correlation is strongest when the two sheets are connected and a superfluid film is present. The presence of uncorrelated avalanches confirms that the superfluid film connection is a crucial mechanism that leads to pore-pore interactions, and thus to correlated avalanches on the two sheets of Nuclepore. This last experiment showed conclusively that correlations between avalanches were not a result of temperature fluctuations or any other external disturbances. If external disturbances caused the pores to drain together, this separate-sample experiment would have continued to show correlated avalanches.

### A. Correlations

We have shown that avalanches are spatially extended and that the avalanche events are correlated on the substrate by the presence of the superfluid film. In order to learn about the *degree* of correlation, we used the concept of covariance as a quantitative measure of the amount of correlation. The covariance  $\Psi$  of two data sets  $x$  and  $y$ , each with  $n$  elements, is

$$\Psi = \frac{1}{n} \sum_{i=1}^n \frac{(x_i - \bar{x})(y_i - \bar{y})}{\sigma_x \sigma_y}, \quad (1)$$

where  $\bar{x}$  is the average of the  $x$  values,  $\sigma_x$  is the standard deviation of the  $x$  values, and similarly for  $\bar{y}$  and  $\sigma_y$ . As we describe below,  $x$  and  $y$  were related to the avalanche behavior on the capacitors being compared. First the avalanche size was determined for every measurement time  $t_i$ . The criteria for avalanches were that the change in  $C$  had to be larger than the noise floor, and that several previous capacitance values before an avalanche had to be stable (within the noise). If no avalanche occurred on  $C1$  ( $C2$ ), a value of 0 was assigned to  $x_i$  ( $y_i$ ). If an avalanche was detected, then a 1 was assigned to  $x_i$  ( $y_i$ ). Depending on how early the run began or how long it lasted, there could be many capacitance measurements before avalanches began or after they ended.

TABLE I. Summary of the covariance of the correlated avalanche behavior for pairs of capacitors.

| Capacitors | Connection | $T$ (K) | $\Psi$ |
|------------|------------|---------|--------|
| $C4-C6$    | porous     | 1.30    | 0.78   |
| $C4-C6$    | porous     | 1.42    | 0.75   |
| $C4-C6$    | porous     | 1.43    | 0.65   |
| $C4-C6$    | porous     | 1.43    | 0.82   |
| $C1-C2$    | porous     | 1.45    | 0.75   |
| $C4-C6$    | porous     | 1.61    | 0.60   |
| $C4-C6$    | porous     | 1.69    | 0.58   |
| $C3-C4$    | nonporous  | 1.30    | 0.68   |
| $C3-C4$    | nonporous  | 1.42    | 0.50   |
| $C3-C4$    | nonporous  | 1.45    | 0.43   |
| $C3-C4$    | nonporous  | 1.61    | 0.21   |
| $C3-C4$    | nonporous  | 1.69    | 0.49   |
| $C3-C4$    | nonporous  | 1.82    | -      |
| $C3-C4$    | nonporous  | 1.98    | -      |
| $C3-C4$    | none       | 1.40    | 0.08   |

Therefore, we limited the range of measurements of  $x_i$  and  $y_i$  to start with the first avalanche and end at the last avalanche. That is, for the sum in Eq. (1),  $i=1$  corresponded to the point of the first avalanche and  $i=n$  corresponded to the last avalanche. A typical set of  $x_i$  and  $y_i$  data used in Eq. (1) consisted of many zeros (times where no avalanches occurred), and only a few ones. This caused  $\bar{x}$  and  $\bar{y}$  to be small. When a correlated avalanche occurred at the  $i$ th point,  $(x_i - \bar{x})(y_i - \bar{y}) > 0$  since  $\bar{x}$  and  $\bar{y}$  were small. This resulted in a positive contribution to  $\Psi$  (independent of the magnitude of the correlated pair). If an avalanche occurred on only one capacitor, there was a smaller negative contribution to  $\Psi$ ; for example,  $-\bar{x}$  when an avalanche occurred on  $C1$  but not  $C2$ . Finally, if there was no avalanche, both  $x_i$  and  $y_i$  were zero, and there was a very small positive contribution  $\bar{x} \cdot \bar{y}$ . The  $\sigma_x$  and  $\sigma_y$  in the denominator were for normalization purposes. The net result is that when  $\Psi \sim 1$ , the avalanches on the different capacitors were well correlated. When  $\Psi \sim 0$ , observed avalanches were not correlated.

The results for the various studies of pairs of capacitors measuring avalanches are summarized in Table I, which lists the pairs of capacitors studied, the temperature, and the resulting values of the covariance. Before looking at the temperature dependence, we first look at all of the data taken near  $T \approx 1.42-1.45$  K. When the two capacitors were on the same sheet of Nuclepore ( $C1-C2$  and  $C4-C6$ ),  $\Psi$  ranged from 0.65 to 0.82. When separated by the nonporous strip of Nuclepore ( $C3-C4$ ),  $\Psi \sim 0.45$ . The nonporous strip reduces the correlation, but does not eliminate it. Since third sound pulses reflected from the nonporous strip (Fig. 7), the reduction in correlation may be due to the attenuation of the amplitude of any superfluid film thickness fluctuations (i.e., third sound) propagating across the strip. When the nonporous strip was removed, the avalanche correlation between the separate pieces of Nuclepore was  $\Psi = 0.08$ ; i.e., very

little correlation between the two capacitors remained. A thermal fluctuation in the cell can induce correlated avalanches, and this may explain the nonzero value.

In an effort to test the validity of this picture experiments with Anopore<sup>13</sup> are underway. Anopore is a material similar in size scale to Nuclepore except that the pores are parallel with few pore-to-pore intersections.<sup>14</sup> Preliminary results<sup>15</sup> indicated that avalanches remain present in the case of Anopore. In the case of Anopore the avalanches are small in size with values for the covariance for experiments with two capacitors on a single Anopore substrate similar to those observed for Nuclepore in the case of the film-only connection (i.e., as seen in the experiments with capacitors C3 and C4). This result is consistent with the notion that the superfluid film plays a predominant role in the case of Anopore, with avalanche sizes limited by the absence of significant pore-pore intersections. These experiments with Anopore are currently ongoing, and will be reported separately.

With the superfluid film established as an important factor in correlating the avalanches, one might expect a dependence on temperature. As  $T \rightarrow T_\lambda$ ,  $\rho_s/\rho \rightarrow 0$ , and the ability of the helium film to support third sound disappears. We have previously seen<sup>1,3</sup> that raising the temperature near  $T_\lambda$  either destroys the presence of avalanches or makes them too small for us to resolve. By measuring  $\Psi$  for both porous (C4–C6) and nonporous (C3–C4) connections at different temperatures, we found a reduced coupling at higher temperatures. In Table I, there is no value for the C3–C4 data in two cases because, as we showed previously,<sup>1,3</sup> avalanches were not present (observable) near  $T_\lambda$  (1.82 and 1.98 K here). The temperature dependence of  $\Psi$  is shown in Fig. 12. The avalanches on the same sheet of Nuclepore were better correlated than those separated by the nonporous strip. For both cases the covariance decreased as the temperature increased. For convenience the temperature dependences of  $\rho_s/\rho$  and  $\sqrt{\rho_s/\rho T}$  are shown in the figure. The predominant temperature dependence of the third sound velocity is given by  $\sqrt{\rho_s/\rho T}$ . Also shown in the figure is the approximate temperature dependence of the amplitude attenuation expected for third sound.<sup>16</sup>

### B. Attempts to stimulate avalanches with third sound

The observation that the avalanches on two porous sheets joined by a nonporous strip remained rather well correlated (Fig. 9) strongly suggests that the superfluid film on the nonporous strip couples the pores on either side, and thus the presence of the superfluid film on the Nuclepore substrate likely is an important factor in pore-pore interaction. The experimental sample (Fig. 6) was designed with third sound drivers and detectors. With these, we were able to propagate single third sound pulses, pulse trains, and continuous waves, while at the same time looking for avalanches. The third sound pulses provided an *in situ* “external” disturbance. We next discuss data that show that single third sound pulses were not effective in the induction of avalanches. Pulse trains of  $\sim 50$  pulses induced avalanches on the Nuclepore where the pulses originated, and sometimes (but not always) a corresponding avalanche appeared across the nonporous strip.

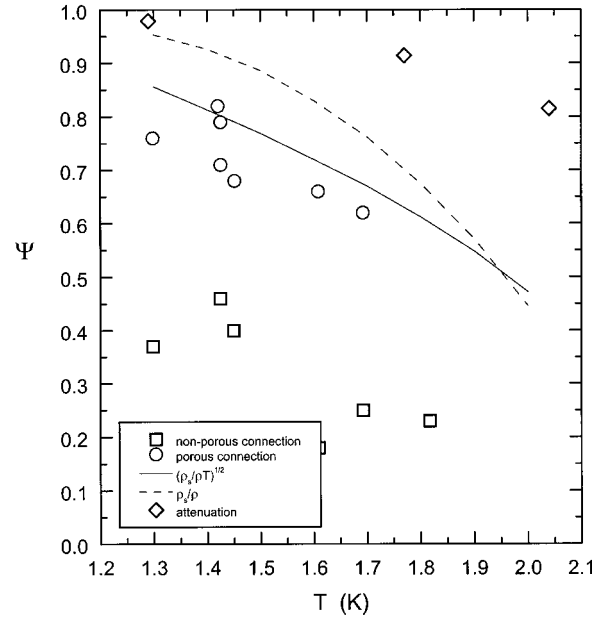


FIG. 12. The temperature dependence of the covariance between two capacitors separated by a porous connection (circles) or a nonporous connections (squares). Also shown in the figure are  $\rho_s/\rho$  (dashed line),  $\sqrt{\rho_s/\rho T}$  (solid line), and the effect of temperature on the amplitude attenuation of third sound (diamonds) (dotted line).

Continuous wave trains of adequate amplitude *suppressed* the size of the avalanches on the Nuclepore substrate where the pulse originated, but did not significantly affect the other Nuclepore substrate.

The first test was to determine if single third sound pulses would induce avalanches. The pores were filled, and then  $^4\text{He}$  was removed until avalanche events began to occur. We monitored C4 while removing  $^4\text{He}$  at  $T=1.425$  K. The pulse generator was configured to allow us to send a single voltage pulse to driver  $E$ , the driver adjacent to C4, where  $R_E=33\Omega$ . As the  $^4\text{He}$  was removed, spontaneous avalanches occurred. When the largest avalanches were occurring spontaneously, we sent a single pulse from driver  $E$  (between spontaneous avalanches), and watched C4 to see if an avalanche was induced by the resulting third sound pulse traveling across the capacitor. We created a total of 11 single pulses with the following amplitudes and widths and (pulse energy values): 2 V, 50  $\mu\text{sec}$  (6.1  $\mu\text{J}$ ); 3 V, 50  $\mu\text{sec}$  (13.6  $\mu\text{J}$ ); 3 V, 100  $\mu\text{sec}$  (27.3  $\mu\text{J}$ ); 4 V, 100  $\mu\text{sec}$  (48.5  $\mu\text{J}$ ), and 5 V, 100  $\mu\text{sec}$  (75.8  $\mu\text{J}$ ). The energy for each was determined from  $E=V^2\Delta t/R$ . None of the single pulses induced an avalanche on C4.

Next we restarted the experiment by refilling the pores and again bringing the experiment to the point where large avalanches appeared spontaneously, and we applied pulse trains to the third sound drivers while monitoring both C3 and C4 for avalanches. Again, the  $^4\text{He}$  was removed continuously at  $T=1.435$  K, so, in addition to induced avalanches, there were spontaneous avalanches. The pulse trains consisted of 3 V, 100- $\mu\text{sec}$  voltage pulses triggered at 43 Hz. At recorded times, we applied these pulses to driver  $A$  ( $R_A$

TABLE II. Results for avalanches on *C3* and *C4* with the application of  $\sim 43$  3 V, 100- $\mu$ sec third sound pulses at  $T = 1.435$  K. The table shows the time corresponding to Fig. 13, the driver, and whether avalanches were induced on *C3* and *C4*.

| <i>t</i> (sec) | Driver   | <i>C3</i> | <i>C4</i> |
|----------------|----------|-----------|-----------|
| 294            | <i>E</i> | no        | yes       |
| 508            | <i>E</i> | no        | yes       |
| 844            | <i>E</i> | yes       | yes       |
| 990            | <i>E</i> | yes       | yes       |
| 1135           | <i>A</i> | yes       | no        |
| 1275           | <i>A</i> | yes       | no        |
| 1490           | <i>A</i> | yes       | no        |
| 2014           | <i>A</i> | no        | no        |
| 2174           | <i>A</i> | yes       | no        |
| 2320           | <i>E</i> | no        | yes       |
| 2580           | <i>E</i> | no        | yes       |
| 2812           | <i>E</i> | no        | yes       |
| 2836           | <i>E</i> | no        | yes       |
| 2912           | <i>E</i> | yes       | yes       |
| 2989           | <i>E</i> | no        | yes       |
| 3102           | <i>A</i> | yes       | no        |
| 3129           | <i>A</i> | yes       | no        |

$=43 \Omega, 20.9 \mu\text{J}/\text{pulse}$ ) or driver  $E(R_E = 33 \Omega, 27.3 \mu\text{J}/\text{pulse})$  for  $\sim 1$  sec, causing  $\sim 43$  pulses to be launched. Table II summarizes the application time, the driver, and whether avalanches were induced on either *C3* or *C4*.

In Fig. 13, the capacitance data for *C3* and *C4* during the course of the application of these pulse trains is shown. The larger circular data points mark the time when the pulse train was applied. On each set of data, the solid circles indicate that the adjacent driver (*A* for *C3*, *E* for *C4*) was activated. The open circles indicate that the further driver (*A* for *C4*, *E* for *C3*) was activated. In every case but one ( $t = 2014$  sec), avalanches were induced on the closest capacitor by the pulse train. When the pulses were applied to *A*, the capacitor across the nonporous bridge *never* avalanched. When they were applied to *E*, three times out of 11 the capacitor across the nonporous bridge did avalanche. We can reach two conclusions. First, a series of pulses will induce an avalanche on a sheet of Nuclepore, but a single pulse of similar amplitude will not. Second, most of the induced avalanches were not correlated with avalanches across the nonporous bridge. Spontaneous avalanches at this temperature, on the other hand, often occur as a correlated pair of avalanches.

We have shown that single pulses do not readily induce avalanches, and that pulse trains can induce avalanches. The next test of the ability of third sound pulses to modify the avalanche behavior was to apply third sound pulses continuously to driver *E*. The continuous pulses were 3-V, 50- $\mu$ sec ( $13.6 \mu\text{J}$ ) voltage pulses triggered at 43 Hz. The capacitance was monitored as  $^4\text{He}$  was drained at  $T = 1.449$  K, and the results are shown in Fig. 14. The ava-

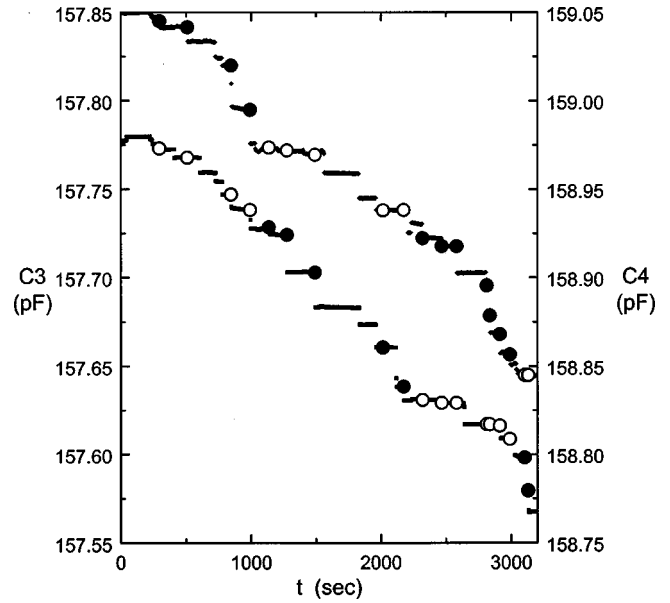


FIG. 13. Results for inducing avalanche with a train of  $\sim 43$  3-V, 100- $\mu$ sec third sound pulses at  $T = 1.435$  K. The left axis (*C3*) corresponds to the lower curve (squares). The right axis (*C4*) corresponds to the upper curve (diamonds). The solid circles mark the time when the adjacent driver sent pulses. The open circles mark the time when the further driver sent pulses. The unmarked avalanches were spontaneous.

lanches on the capacitor adjacent (*C4*, circles) to the active third sound driver appear “washed out,” while those on the capacitor across the nonporous strip (*C3*, squares) appeared distinct. When 2-V, 50- $\mu$ sec ( $4.7-\mu\text{J}$ ) continuous pulse trains were applied to driver *A*, the reverse occurred: the

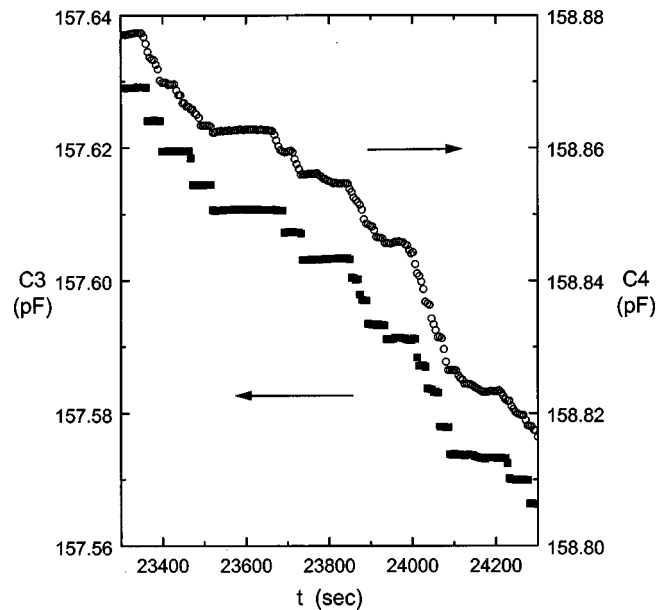


FIG. 14. Avalanches on *C3* and *C4* at  $T = 1.4488$  K while 3 V, 50- $\mu$ sec ( $13.6 \mu\text{J}$ ) third sound pulses were continuously applied to driver *E*. The signal from *C3*, across the nonporous strip from *E*, appears similar to other avalanche traces. The signal from *C4*, adjacent to *E*, appears “washed out.”

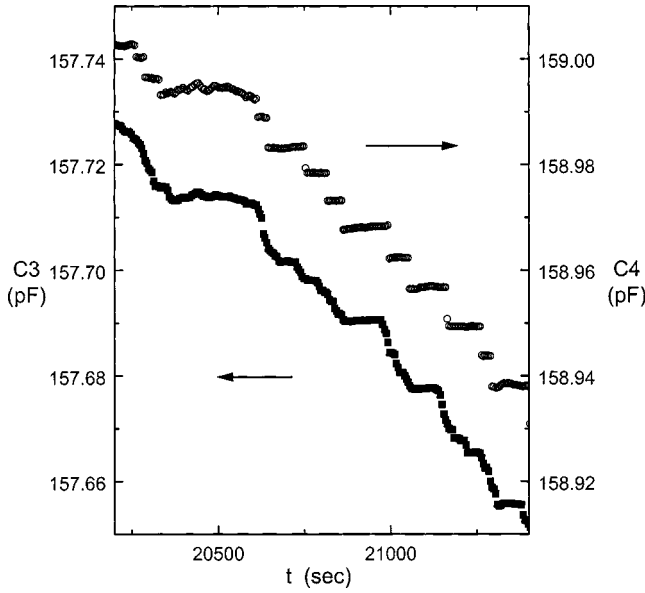


FIG. 15. Avalanches on  $C3$  and  $C4$  at  $T=1.4480$  K while 2-V, 50- $\mu$ sec (4.7  $\mu$ J) third sound pulses were continuously applied to driver A. This time, the signal from  $C3$ , adjacent to A, appears washed out.

avalanches on  $C3$  were washed out, as shown in Fig. 15. It appears that the presence of the perturbation introduced by the presence of continuous third sound stimulates the production of vary many small (unresolvable) avalanches or continuous draining in a manner that prevents the system from producing large avalanches. Apparently continuously applied third sound stimulates small avalanches, and prevents the “buildup” of avalanche size by releasing avalanches before a significant number of filled pores can reach a condition of metastability as the chemical potential is reduced. The result of this phenomenon appears to be that since no large avalanches can appear on one Nuclepore substrate in the presence of a continuous third sound stimulation, no large event is available to cause a film fluctuation large enough to have a significant effect by the time it propagates across the nonporous bridge. It is apparently also the case that avalanches spontaneously created on the region of the sample with no third sound are unable to stimulate avalanches on the other region of the substrate because the pores there have been “tickled” away from metastability by the applied third sound.

#### IV. IMPLICATIONS OF THE ROLE OF THE SUPERFLUID FILM

With the importance of the superfluid film apparently well established, we discuss a number of our observations in terms of the role of the superfluid. When an avalanche occurs, the liquid  $^4\text{He}$  that drains from the pores is removed by superfluid film flow and perhaps also by the evaporation of  $^4\text{He}$  atoms to vapor. To estimate the shortest likely time for fluid draining, we consider the case of fluid flow draining at  $T=0$  K. First we show that the draining time for a single pore is very short; then we discuss the  $^4\text{He}$  draining from the

Nuclepore sheet when many pores drain.

The time for a single pore to drain,  $\Delta t$ , will be limited by the perimeter of the pore opening. This time is  $\Delta t = \pi R^2 l / 2\pi R d v$ , where  $R=100$  nm is the pore radius,  $l \approx 10$   $\mu$ m is the pore length (ignoring the enhanced length of tilted pores),  $d$  is the film thickness on Nuclepore, and  $v$  is the velocity of the moving film. For simplicity, here we have taken  $\rho_s/\rho=1$ . If the pore drains from both sides, there will be an additional multiplicative factor of 0.5. Avalanches occur in 200-nm Nuclepore on the steep portion of the primary desorption curve, where  $\mu \sim -0.015$ . The corresponding film thickness on Nuclepore is  $d \approx (-50 \text{ layers}^3 \text{ K}/\mu)^{1/3} \approx 14.9$  atomic layers ( $\approx 5.36$  nm). The fastest pore draining must occur when the  $^4\text{He}$  film flows at the critical velocity in the neck of the pore where the diameter is thought to be smallest. Telschow *et al.*<sup>17</sup> showed that the film critical velocity at  $T=1.5$  K, for a film thickness range of 7 - 15 atomic layers, is  $v_c \approx 200$  cm/sec. Using this value results in  $\Delta t \approx 4.7 \times 10^{-4}$  sec as the time required to drain a typical single pore. A single pore can drain much faster than we can measure with the Andeen-Hagerling capacitance bridge. In this argument we have neglected the normal fluid. Since only the superfluid flows, complete draining in the system at  $T > 0$  will be somewhat slower, as the entropy associated with the normal fluid must be removed.

Now we consider the effect of *many* pores draining, as happens for an avalanche. The volume of liquid that drains must be removed via the perimeter of the Nuclepore sample (or be assisted by evaporation). A volume  $\Delta V$  (resulting from the draining of many pores), removed by the superflow of a film through a perimeter  $p$  (at the edge of the Nuclepore), occurs in time

$$\Delta t = \frac{\Delta V}{p d v_s}, \quad (2)$$

where  $d$  is the film thickness and  $v_s$  is the superfluid velocity. Avalanches occurred where the film thickness on Nuclepore was  $d=14.9$  layers. For an avalanche involving  $N$  pores, the volume of  $^4\text{He}$  is  $\Delta V = N \pi R^2 l$ , where  $R=100$  nm and  $l=10$   $\mu$ m are the radius and length of the cylindrical pore. For the typical significant avalanche jumps (where the duration of the avalanches was measured,<sup>1,3</sup>)  $\Delta C \sim 0.1$  pF, and  $N = 2.5 \times 10^7$  pores. The Nuclepore sample was clamped to a Cu frame at the corners, so we conservatively estimate the perimeter of the Nuclepore over which the film flow could leave the Nuclepore to be on the order of  $p=1$  cm. Using these numbers, the time necessary for this volume of  $^4\text{He}$  to be removed from the sample is 0.7 sec. Typically for such an avalanche we measured a time duration of 1.3 sec,<sup>1,3</sup> similar to the predicted removal time of the volume of  $^4\text{He}$  through the sample perimeter at the critical velocity. The observed avalanche events represent a relatively slow phenomenon, a phenomenon not limited by either the draining time of single pores, but possibly limited by the the flow of helium from the substrate to the local environment.

Our experiments show that avalanches occur and that the superfluid  $^4\text{He}$  film can couple pores over long distances. We have found that the superfluid draining of the pores may be

enabled by the superfluid film as an interaction mechanism, and also that pore-film-pore interactions may enhance the duration of the avalanches. Using capacitors, we have not yet had the resolution to observe the actual dynamics of the film motion during an avalanche event. That is, we have not yet done an experiment with, for example, a collection of distributed small capacitors that would allow us to study the time *and* spatial evolution of an avalanche event as it presumably washes across the substrate. If avalanches are relatively slow events, such an experiment should allow a spatial resolution of the development of an avalanche event as it crosses the substrate. It is possible that perimeter effects limit the flow of fluid from the substrate, and lengthen the apparent duration of the avalanches. New experiments of different design will be required to check for this.

Finally, we discuss recent theoretical work of Guyer and McCall<sup>18</sup> on superfluid avalanches in Nuclepore. In the model developed by Guyer and McCall,<sup>18</sup> an avalanche event starts with the draining of a single pore. In the primary process, the fluid from this pore propagates across the system as a third sound wave. The amplitude disturbance accompanying the third sound wave induces other pores that were close to the draining instability to drain immediately. The secondary process occurs when these pores, induced to drain by the first pore, themselves propagate third sound waves and cause other pores to drain. This is similar to our picture of sequential pore draining.<sup>1,3,19</sup> After these draining events, the extra fluid on the Nuclepore surface raises the local chemical potential with an increased film thickness on the surface of the Nuclepore. As a result of the increased chemical potential, the avalanche ceases. Quantitatively, using the pore size and spectrum of radii for Nuclepore and the range of chemical potential predicted by an invasion percolation process, they find avalanche sizes on the order of one to tenth those observed our experiment. We expect that some combination of pore-film-pore *and* direct pore-pore interaction<sup>1,3,19</sup> is likely at work and both contribute. When both are present the avalanches are large, but when only the film mechanism is present the avalanches are smaller. As noted earlier, in an effort to test the validity of this picture experiments with Anopore<sup>13</sup> are underway. This simple model of superfluid avalanches addresses the open problem of the dynamics involved in the draining of many pores in a short time. We have shown that single third sound pulses with energies from  $6.1 \mu\text{J}$  to  $75.8 \mu\text{J}$  do not typically induce avalanches. This result is in conflict with the simple primary event proposed by Guyer and McCall in the superfluid avalanche model, where a single third sound event triggers the avalanche. However, pulse trains do stimulate avalanches, and perhaps this enhanced stimulation is consistent with the model.

## V. SUMMARY

In this work and our earlier work,<sup>3</sup> we presented a series of measurements on the draining of  $^4\text{He}$  from Nuclepore with both 200- and 30-nm diameter pores. Single capacitor measurements showed that sudden steps occurred as  $^4\text{He}$  was removed. These steps corresponded to large groups of

pores draining on time scales of the order of 1 sec. The measured capacitance steps indicated that groups of pores ranging in number from  $2 \times 10^4$  to  $3 \times 10^7$  were involved in the avalanche events. Measurements with two capacitors on the same sheet of Nuclepore showed that these avalanche events were spatially extended, and for the case of small size avalanches involved only a low-density of pores across the sample. The next series of experiments showed that capacitors on separate sheets of Nuclepore connected by a nonporous strip remained correlated. When the strip was removed, the avalanche events were uncorrelated. This measurement indicated that the superfluid film that bridged the two sheets of Nuclepore across the nonporous strip plays a significant role in coupling the avalanche events.

From the initial surprising observation of sudden jumps in the capacitance as  $^4\text{He}$  drained from the pores in Nuclepore, it seemed likely that the superfluid was a factor. We are not aware of observations of avalanches in the draining of any other porous system as normal fluids drain, no doubt due to the presence of viscosity and the consequent long time constants. We have considered a number of mechanisms for avalanches. In the first mechanism, the avalanches occur as an invasion percolationlike event, where large groups of directly connected pores drain (and empty pores replace pores previously filled), and with the high mobility of the superfluid, they can be observed. This was shown to be at most only a part of the story by the observations on multiple capacitor substrates. In these observations, all of the avalanche events were spatially extended, even the small ones, and avalanches remained substantially correlated even without the porous connection. In the second mechanism, connectivity remains important, but for avalanches to occur, some kind of superfluid dynamics is critical for long range coupling and quick removal of the fluid. The final possible mechanism is that superfluid is the only requirement for avalanches, and that connectivity plays no role. With our experiments, we have shown that the first is inadequate to explain the data. In order to establish the role of connectivity, studies are planned of the primary desorption curve of Anopore, a porous material where the pores are reported to have limited internal connection. Preliminary studies<sup>15</sup> suggest that for Anopore avalanches are indeed present, although reduced in size from those seen on Nuclepore, a result consistent with the model in which the superfluid helium film enables the avalanches. The picture that emerges is that the presence of the film is important, but interconnections enhance the amplitude of the avalanches.

## ACKNOWLEDGMENTS

We have benefited from conversations with K. Dahmen and R.A. Guyer. This work was supported by the National Science Foundation through Grant Nos. DMR 97-29805 and DMR 98-19122 and by research trust funds administered by the University of Massachusetts Amherst.

## APPENDIX A

In this appendix we present evidence of the noise introduced by the electronic switch used to switch the capacitance

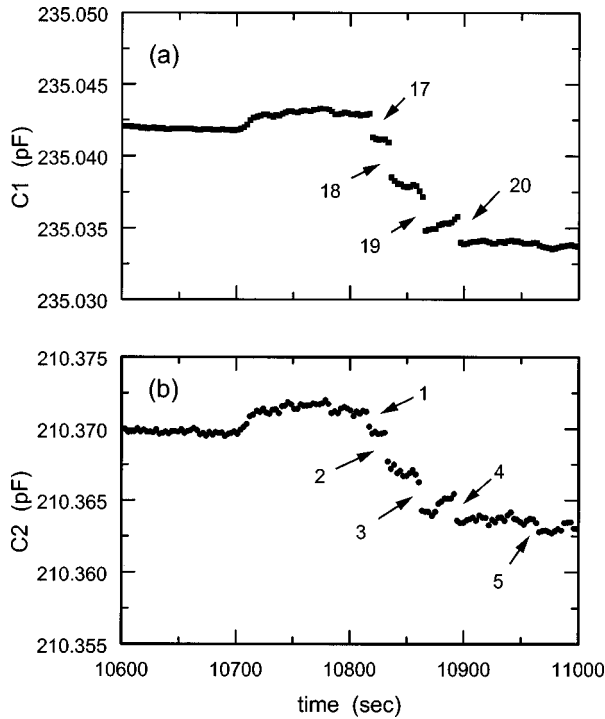


FIG. 16. An example of the noise introduced by the capacitor switch for the double-capacitor run as the pores begin to drain. Avalanches were clear on  $C1$  in (a), while in (b) extra noise was introduced by the switch, making it harder to identify the smaller avalanches. The increasing and decreasing drifts in the capacitance were also due to the switch. The numbers refer to jumps meeting the criteria to be considered avalanches.

bridge between the two measuring capacitors  $C1$  and  $C2$ . We also show that the strong correlation in avalanche behavior for the two capacitors was *not* introduced by the presence and operation of the switch. We do this by removing the switch and making simultaneous measurements of the two capacitors using two separate and independent bridges.

The noise introduced by the switch can be seen by comparing the single capacitor data from our earlier work<sup>1</sup> to data taken with the switch. Since this noise is obvious before draining begins on the primary desorption, the effect of the switch was observed in the global hysteresis loops.<sup>2</sup> These data are much noisier than the earlier data<sup>1</sup> without the switch. It is also the case that of the two capacitors  $C1$  and  $C2$ ,  $C2$  displayed a bit more intrinsic noise than did  $C1$ . Both this intrinsic difference and the effect of the switch noise are shown in Fig. 16 at the onset of draining. One of the channels (measuring  $C2$ ) introduced noise with a period comparable to (or shorter than) the time between the data points,  $\sim 10$  sec. In Fig. 16(a), the data from  $C1$  had clear, sharp avalanches. The numbers 17–20 denote avalanches that are large enough to be counted. In Fig. 16(b), for the same range, data from  $C2$  include more scatter in the data. Due to the increased scatter, the avalanche near  $t = 10800$  sec was the first clear avalanche that was counted. The net result was that  $C1$  appeared to have more avalanches (96) than  $C2$  (79); it is likely that this is because it was

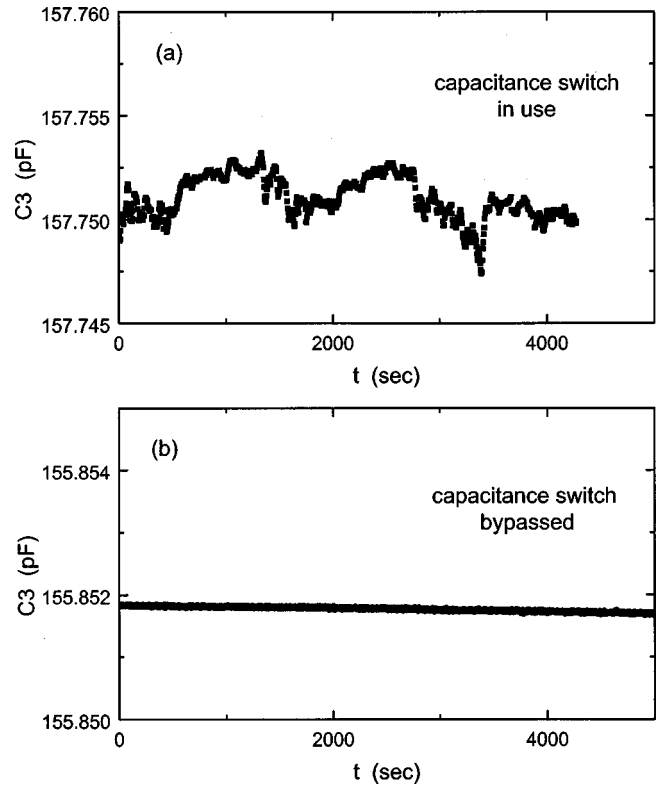


FIG. 17. Effect of the capacitance switch on avalanche run before draining occurred. In (a), the switch was used ( $T = 1.299$  K). In (b), the switch was bypassed ( $T = 1.298$  K). The presence of the switch greatly increased the noise.

easier to identify avalanches on  $C1$ . In both cases the larger scale noise and drifts are due to the switch.

A more dramatic example of the noise induced by the capacitor switch is shown in Fig. 17. This data were taken for the sample which we have denoted  $C3$ . In Fig. 17(a) we show an avalanche run before draining commenced with the switch in place and operating. The noise level is  $\delta C \sim 5 \times 10^{-3}$  pF. In Fig. 17(b), we show an avalanche run before draining began for the same capacitor but this time the switch was bypassed (i.e., removed from the signal path), and the noise level was reduced to  $\delta C \sim 2 \times 10^{-4}$ . The switch was necessary for long-term measurements that involved multiple capacitors, but a substantial penalty was paid with an increased noise level. The switch was adequate to measure the behavior of the large avalanches, and allows us to reach the conclusions we sought for this set of experiments.

One thing the switch did *not* do was induce avalanches just by switching, or by its presence. We proved this by simultaneously measuring one pair of capacitors with two different capacitance bridges with the switch removed from the system. This measurement was made with the same sample that held capacitors  $C4$  and  $C6$ , with these capacitors located on the same sheet of Nuclepore as was the case for  $C1$  and  $C2$ . The first bridge was the self-balancing Andeen-Hagerling 2500A operating at 1000 Hz. This bridge was used for all of the other measurements we report in this paper. The second bridge was a General Radio 1615-A capacitance

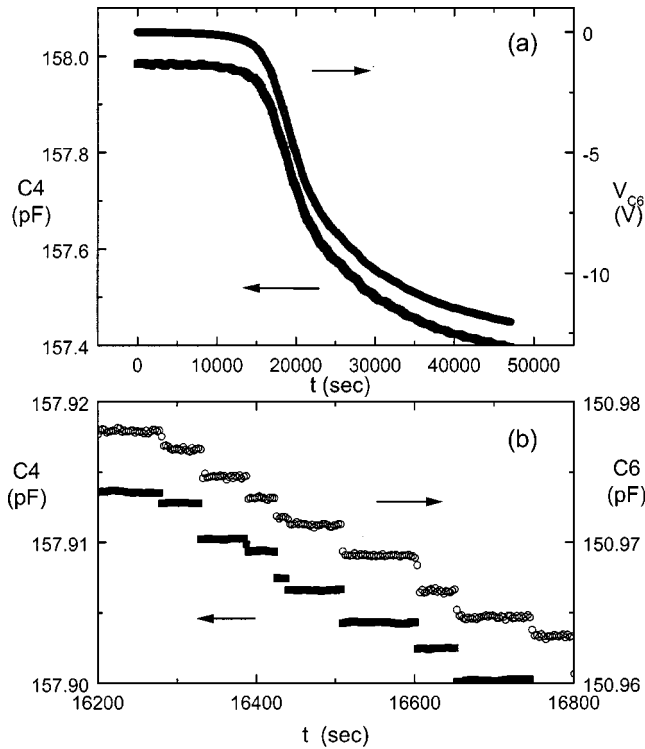


FIG. 18. Avalanche correlations using two capacitance bridges (no switch). The squares are for  $C4$  (data taken with the Andeen Hagerling bridge) and the circles for  $C6$  (data taken independently with a General Radio 1615A bridge). In (a) we show the full run, reporting the measured voltage offset of the lock-in for  $C6$ . In (b) a magnified view of the curves confirms simultaneous avalanches. Here the lock-in voltage has been converted to capacitance.

bridge driven by a lock-in detector with a reference signal of 1-V rms at 710 Hz. These results, similar to those shown in Fig. 2, are shown in Fig. 18, and confirmed the simultaneous avalanches. The correlation between data from  $C4$  and  $C6$  using two independent bridges proves that the switch was not responsible for inducing avalanches on both capacitors at the same time; the switch was not present when these data (Fig. 18) were taken.

## APPENDIX B

In order to identify the multiple peaks in Fig 7(b) (4160, 5300, 6300, and 7250  $\mu\text{sec}$ ) as reflections, we used the geometry of the sample, which is shown in Fig. 19 as a schematic diagram. The direct path from  $E$  to  $D$  has a length  $L$ . The three reflections have lengths  $y+L$  (path 2),  $x+L$  (path 3) and  $x+y+L$  (path 4). The total path length due to (path 1) + (path 4) and (path 2) + (path 3) will each equal  $x+y+2L$ . For the above reflections, we add the correspond-

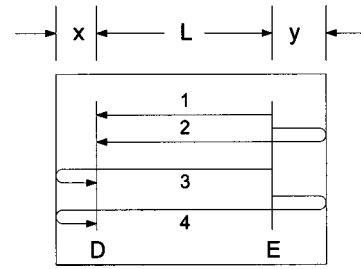


FIG. 19. Sketch for identifying reflections. The direct path (1) has a length  $L$ . The three reflection paths that we consider are path 2 with length  $y+L$ , path 3 with length  $x+L$ , and path 4 with length  $x+y+L$ .

ing times and find (path 1)+(path 4)=11410  $\mu\text{sec}$  and (path 2)+(path 3)=11600  $\mu\text{sec}$ . Another equal path length is (path 3)-(path 1)= $x$  and similarly, (path 4)-(path 2)= $x$ . The corresponding arrival time for the pulses in Fig. 7 were (path 3)-(path 1)=2140  $\mu\text{sec}$  and (path 4)-(path 2)=1850  $\mu\text{sec}$ . Finally, (path 4)-(path 3)= $y$  and (path 2)-(path 1)= $y$ . The arrival times were (path 4)-(path 3)=950  $\mu\text{sec}$  and (path 2)-(path 1)=1140  $\mu\text{sec}$ . We do not actually know from the reflections if the routes (path 2) and (path 3) in the figure correspond to the second and third reflections, but the relationship between the arrival times was consistent with the four different paths shown in Fig. 19.

The arrival time of the pulses is consistent with the index of refraction of third sound on Nuclepore reported by Godshalk *et al.*,<sup>5</sup> and with the dimensions of our sample. Godshalk *et al.* found  $\tau_s/\tau_g \sim 1.1$  (index of refraction for nonporous Nuclepore compared to glass) and  $\tau_p/\tau_s \sim 3.0$  (index of refraction for nonporous to porous Nuclepore) for  $d_g = 9.2$  layers. From Fig. 7 we find

$$\frac{\tau_{glass}}{1.02 \text{ cm}} \bigg/ \frac{\tau_{E-D}}{1.43 \text{ cm}} = 3.5.$$

This is the combined index of refraction for porous Nuclepore compared to glass, and should be compared  $1.1 \times 3.0 = 3.3$  from Smith *et al.* The velocity of third sound on the porous Nuclepore was  $v_p = 1.43 \text{ cm}/4160 \mu\text{sec} = 344 \text{ cm/sec}$ , and the velocity on smooth Nuclepore was  $v_s = 3.5v_p/1.1 = 1095 \text{ cm/sec}$ . Since the pulse from  $A$  to  $D$  travels across 1.8 cm porous Nuclepore and 0.7 cm of nonporous Nuclepore we would predict the arrival time

$$\tau_{predicted} = \frac{0.7 \text{ cm}}{1095 \text{ cm/sec}} + \frac{1.8 \text{ cm}}{344 \text{ cm/sec}} = 5870 \mu\text{sec}.$$

This is in reasonable agreement to the measured  $\tau_{A-D} = 6100 \mu\text{sec}$ .

\*Present address: Sandia National Laboratories, Albuquerque, New Mexico 87185.

<sup>1</sup>M.P. Lilly, P.T. Finley and R.B. Hallock, Phys. Rev. Lett. **71**, 4186 (1993).

<sup>2</sup>M.P. Lilly and R.B. Hallock, Phys. Rev. B **63**, 174503 (2001).

<sup>3</sup>M.P. Lilly and R.B. Hallock, Phys. Rev. B **64**, 024516 (2001).

<sup>4</sup>K. R. Atkins and I. Rudnik, *Progress in Low Temperature Physics*, edited by C. J. Gorter (North-Holland, Amsterdam, 1970), Vol. VI.

<sup>5</sup>K.M. Godshalk, D.T. Smith, and R.B. Hallock, Phys. Rev. B **36**,

202 (1987). Figure 2 of this paper shows scanning electron microscope images of the surface of Nuclepore and also of a side-cut section of the Nuclepore. The nominal pore diameter of the Nuclepore in these images is the same as that used in this work.

<sup>6</sup>For the purpose of this estimation, we take the typical avalanche size to be 0.007 pF. Capacitors  $C1$  and  $C2$  have an area of  $\sim 1$  cm<sup>2</sup>, and include  $3.5 \times 10^8$  pores (the approximate pore density for 200-nm pore diameter Nuclepore is  $3.5 \times 10^8$  pores/cm<sup>2</sup>). Thus, such an avalanche involves  $n = (7 \times 10^{-3} \text{ pF})(3.5 \times 10^8 \text{ pF}/1 \text{ cm}^2) = 2.5 \times 10^6$ . Thus  $l \sim (A/N)^{1/2} = (1/2.5 \times 10^6)^{1/2} = 6.4 \text{ } \mu\text{m}$ .

<sup>7</sup>Note the weak dependence on the ratio of the avalanche sizes with the amount of <sup>4</sup>He in  $C1$  shown in Fig. 5(a). This slope is consistent with our earlier observations. Here, for  $C1 \sim 235$  pF, the ratio was, on average, a little larger than 1. Avalanches on  $C1$  were larger. In Fig. 3, we see that in the correlated pairs  $\Delta C1$  (avalanche on  $C1$ , square) was usually larger than  $\Delta C2$  (avalanche on  $C2$ , circle) when  $C - C_{full} \sim 0$ . In Fig. 4 we see that more <sup>4</sup>He drained from  $C1$  (the difference decreased) as avalanches first began. In Fig. 5(a), for  $C1 \lesssim 234.7$  pF, the avalanches on  $C2$  were, on average, larger. In Fig. 3, for  $C - C_{full} \lesssim -0.3$  pF,  $\Delta C2$  (avalanche on  $C2$ , circle) was usually larger. The difference in Fig. 4 was increasing. All of these observations were consistent with more <sup>4</sup>He draining from  $C1$  as draining commenced.

<sup>8</sup>M.P. Lilly, A.H. Wootters, and R.B. Hallock, Phys. Rev. Lett. **77**, 4222 (1996).

<sup>9</sup>For a discussion on the use of third sound to determine the chemical potential and the approximate film thickness, see Ref. 2.

<sup>10</sup>D.T. Smith, J.M. Valles, Jr., and R.B. Hallock, Phys. Rev. Lett. **54**, 1528 (1985).

<sup>11</sup>If the Nuclepore structure is such that it is not homogeneous on a relatively large length scale, it might be the case that the pore size distribution in the vicinity of one capacitor plate might differ a bit from that in the vicinity of the other. This could cause draining on one to lead or lag that on the other. We have no reason to doubt the spatial homogeneity of Nuclepore and the manufacturer does not indicate such inhomogeneity is present.

<sup>12</sup>The only potential connections that remained after the nonporous bridge was removed were (1) the helium vapor in the experimental cell due to the finite vapor pressure, and (2) the very weak film connection created by the helium film that decorated the fine-wire electrical leads to  $C3$  and  $C4$ .

<sup>13</sup>Whatman Industries Ltd., Maidstone, England and Tewksbury, MA.

<sup>14</sup>G.P. Crawford, L.M. Sgteele, R. Ondris-Crawford, G.S. Iannacchione, C.J. Yeager, J.W. Doane, and D. Finotello, J. Chem. Phys. **96**, 7788 (1992). This paper also includes images of the surface of Nuclepore and some characterization information.

<sup>15</sup>A.H. Wootters, M.P. Lilly, and R.B. Hallock, J. Low Temp. Phys. **110**, 561 (1998).

<sup>16</sup>K.L. Telschow, R.K. Galkiewicz, and R.B. Hallock, Phys. Rev. B **14**, 4883 (1976). It should be noted that the temperature dependence shown here is for saturated films, i.e., films thicker than those used in these Nuclepore experiments.

<sup>17</sup>K.L. Telschow, I. Rudnick and T.G. Wang, Phys. Rev. Lett. **32**, 1292 (1974).

<sup>18</sup>R.A. Guyer and K.R. McCall, J. Low Temp. Phys. **111**, 841 (1998).

<sup>19</sup>M.P. Lilly and R.B. Hallock, in *Dynamics in Small Confining Systems II*, edited by J. M. Drake, J. Klafter, R. Kopelman, and S.M. Troian, MRS Symposia Proceedings No. 366 (Materials Research Society, Pittsburgh, 1995), p. 241.